Supplementary Information:
The effect of temperature and relative humidity on secondary organic aerosol formation from ozonolysis of Δ^3-carene

D. Thomsen[1,†], E. M. Iversen[1,†], J. T. Skønager[1], Y. Luo[2], L. Li[3], P. Roldin[4,6], M. Priestley[3,7], H. B. Pedersen[5], M. Hallquist[3], M. Ehn[2], M. Bilde[1,*] and M. Glasius[1,*]

[1] *Department of Chemistry, Aarhus University, 8000 Aarhus C, Denmark*
[2] *Institute of Atmospheric and Earth System Research (INAR), University of Helsinki, 00014 Helsinki, Finland*
[3] *Department of Chemistry, University of Gothenburg, 41296 Gothenburg, Sweden*
[4] *Division of Physics, Lund University, 22100 Lund, Sweden*
[5] *Department of Physics, Aarhus University, 8000 Aarhus C, Denmark*
[6] *IVL Swedish Environmental Research Institute, 21119 Malmö, Sweden*
[7] *IVL Swedish Environmental Research Institute, 41133 Gothenburg, Sweden*

† These authors contributed to the manuscript equally.
* Corresponding authors

This supplementary information contains seven sections. Section 1 presents a schematic of the instrument placements during ACCEPTO and sampling cycles for instruments not sampling continuously. Section 2 presents the method used for wall-loss correction. Section 3 shows experimental overview plots presenting particle number concentrations, particle mass concentrations, particle mode diameter, ozone concentrations, temperature and relative humidity. Section 4 shows background measurements of sulfuric acid inside the atmospheric simulation chamber. Section 5 shows the evolution of moderately oxygenated species at different relative humidities. Section 6 describes the details of the offline analysis (UHPLC-QTOF-MS method and detection limits for analytes used as surrogate standards) and time-evolution plots of ozonolysis products as mass fractions and the time-evolution plot of the concentration of *cis*-3-caronic acid. Section 7 shows the ADCHAM model results for experiments 0A, 20A, and 20B and the modelled SOA yields for experiments 0A, 10A, 10B, 20A and 20B.

The data is available from the ATMO-ACCESS Database of Atmospheric Simulation Chamber Studies under the following DOIs.

Date	ID	DOI
220202	0A	https://doi.org/10.25326/V4X9-EX29
220113	10A	https://doi.org/10.25326/62Y1-3K47
220204	10B	https://doi.org/10.25326/6XQN-5852
220427	10C	https://doi.org/10.25326/BF7F-F767
220124	10D	https://doi.org/10.25326/DT8P-XF52
220131	10E	https://doi.org/10.25326/D1A9-G032
220111	20A	https://doi.org/10.25326/TBWC-R133
220205	20B	https://doi.org/10.25326/MWVJ-TT47

SI-1 Flow from chamber during experiments

This section presents the instrument placements around the AURA chamber and flows, which they remove air from the chamber with.

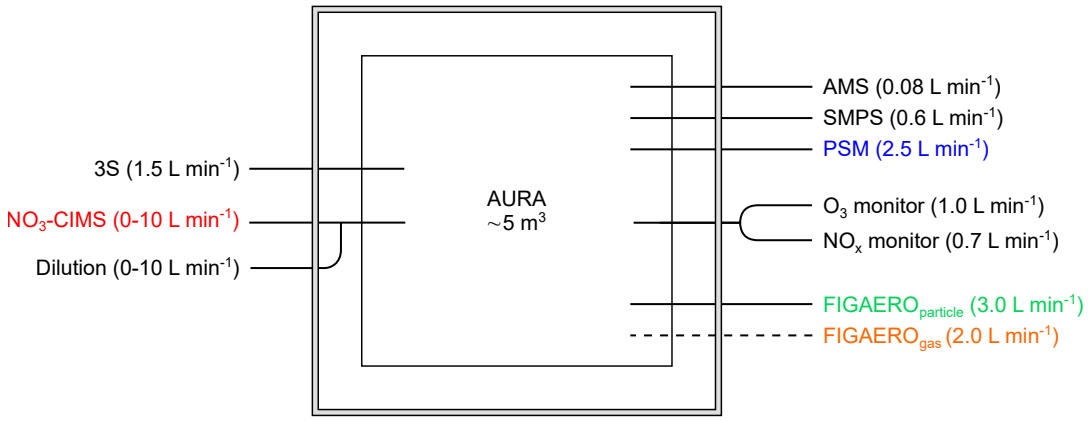

Figure S.1 Schematic of the AURA chamber and how the instruments were placed. Instruments in black were running for the entire experiment. Instruments in colors followed the sampling cycles in Figure S.2. The dashed line represents a Teflon tube for sampling gases with the FIGAERO-CIMS. The solid lines represent stainless steel sampling lines. The double square represents the temperature-controlled room.

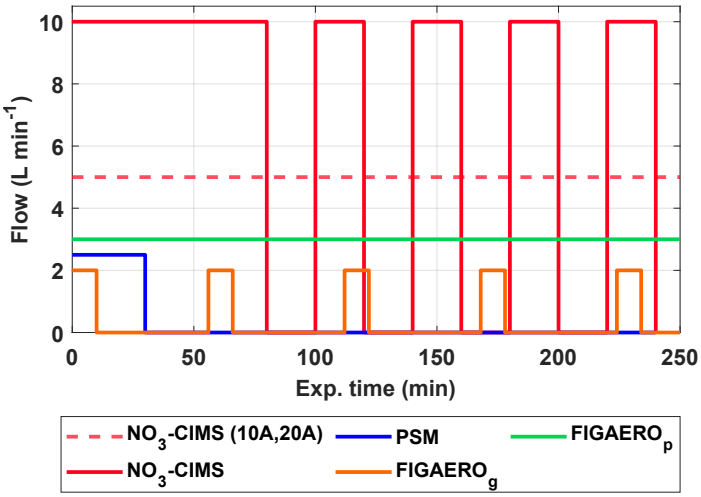

Figure S.2 Sampling cycles for the instruments NO_3-CIMS, FIGAERO-CIMS, and PSM. In experiments 10A and 20A the NO_3-CIMS sampled continously with a flowrate of $5\,\mathrm{L\,min^{-1}}$ with a dilution flow of $5\,\mathrm{L\,min^{-1}}$ (dashed line). In all other experiments, the NO_3-CIMS sampled periodically and the dilution flow for the NO_3-CIMS ran the opposite cycle of the NO_3-CIMS (full line).

SI-2 Wall-loss correction

During simulation chamber experiments, particles are continuously lost to the chamber walls. To correct for this unwanted effect, an exponential fit is usually made in a part of the experiment, where it is expected, that only wall loss happens (i.e. no nucleation, particle growth etc.). The exponential fit gives the particle wall loss rate constant, k_w, which is used to correct for particle wall loss. In this work we build upon the method by Pathak et al. [1], briefly described here: The corrected mass concentration, $M_{corr}(t)$, was calculated as

$$M_{corr}(t) = M(t) + k_w \int_0^t M(t)\ \mathrm{d}t. \tag{S.1}$$

In practice, the integral was calculated as a sum of mass concentrations and multiplied with the average time between two measurements, t_{sample}

$$M_{corr}(t) = M(t) + k_w \sum_{i=0}^{t} M_i\ t_{sample}. \tag{S.2}$$

In VOC oxidation experiments like those carried out in this work, the period where the exponential fit is done is usually after the SOA production has stopped and particle number or mass has reached a maximum. When exactly to start the fit may rely on a subjective process in determining when the SOA production has stopped. In this work, a more objective approach was used. Instead of manually choosing which period to use for wall loss correction, a certain period was selected. For each data point in the period, an exponential fit was carried out using all times from the certain data point to the end of the experiment. Each of the exponential fits yielded an r^2-value. The finally selected exponential fit used to correct for particle wall-loss, was the one with the highest r^2-value. The start of the period was the time point where the SMPS mass concentration reached the maximum value of the experiment. The end-point of the selected period was 20 data points before the end of the experiment. This ensured that at least 20 data points would make up the exponential fit used to correct for particle wall loss. In experiment 10B, the mass concentration reached a maximum very late. Hence the end-point of the fitting period was set to 10 data points before the end of the experiment. In practice, the best exponential fit would usually start shortly after the peak in mass concentration. Figure S.3 shows an example of the correction. This procedure for particle wall loss correction was carried out for the SMPS mass concentrations for all experiments.

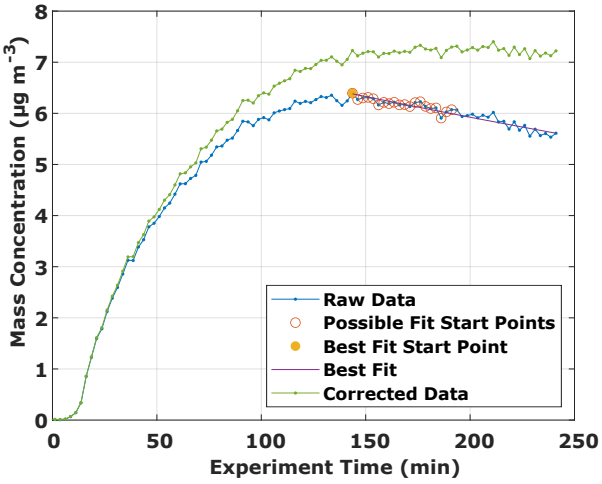

Figure S.3 Wall-loss correction example for experiment 20B made with the best exponential fit.

SI-3 Experimental overview

Experimental overviews showing the time evolution of the particle formation and growth, the decay in ozone concentration, and the course in temperature and relative humidity are presented in Figure S.4–Figure S.7. In all figures, panel (I) shows the SMPS particle number concentration in # cm^{-3}, the PSM particle number concentration in # cm^{-3}, and the ozone concentration in ppb. (II) shows the SMPS mass concentration in µg m^{-3} and the SMPS mode diameter in nm. (III) shows the temperature in °C and the relative humidity in %. After the injection of Δ^3-carene, a decrease in the ozone concentration is observed consistent with the consumption by reaction with Δ^3-carene. The temperature remains constant throughout all experiments, except at 0 °C, where small temperature fluctuations (<1 °C) are observed arising from the cooling system of the atmospheric simulation chamber. The relative humidity increases slightly (from 0 % to 5.3 % over 240 min) during experiments with RH 0 %. This has previously been observed in the AURA atmospheric simulation chamber [2–4] and is ascribed to the permeability of Teflon film to water vapour. In experiments 10D and 10E, the relative humidity was ∼80 % when injecting Δ^3-carene. With time, a decrease in relative humidity (8 % over 240 min) is observed. This is likely due to air entering the Teflon bag from the surrounding air in the cooling room with a lower RH (∼30 %).

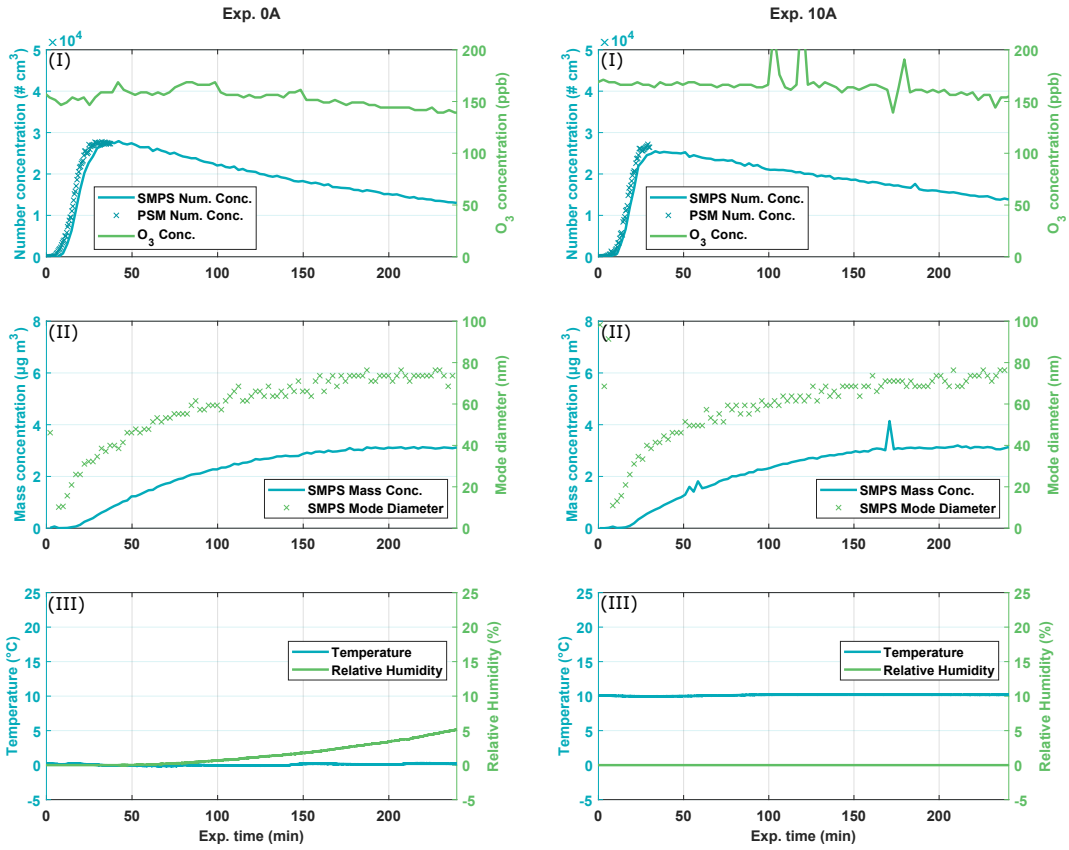

Figure S.4 (I) SMPS particle number concentration in # cm^{-3}, PSM particle number concentration in # cm^{-3}, and ozone concentration in ppb. **(II)** SMPS mass concentration in µg m^{-3} and SMPS mode diameter in nm. **(III)** Temperature in °C and relative humidity in %.

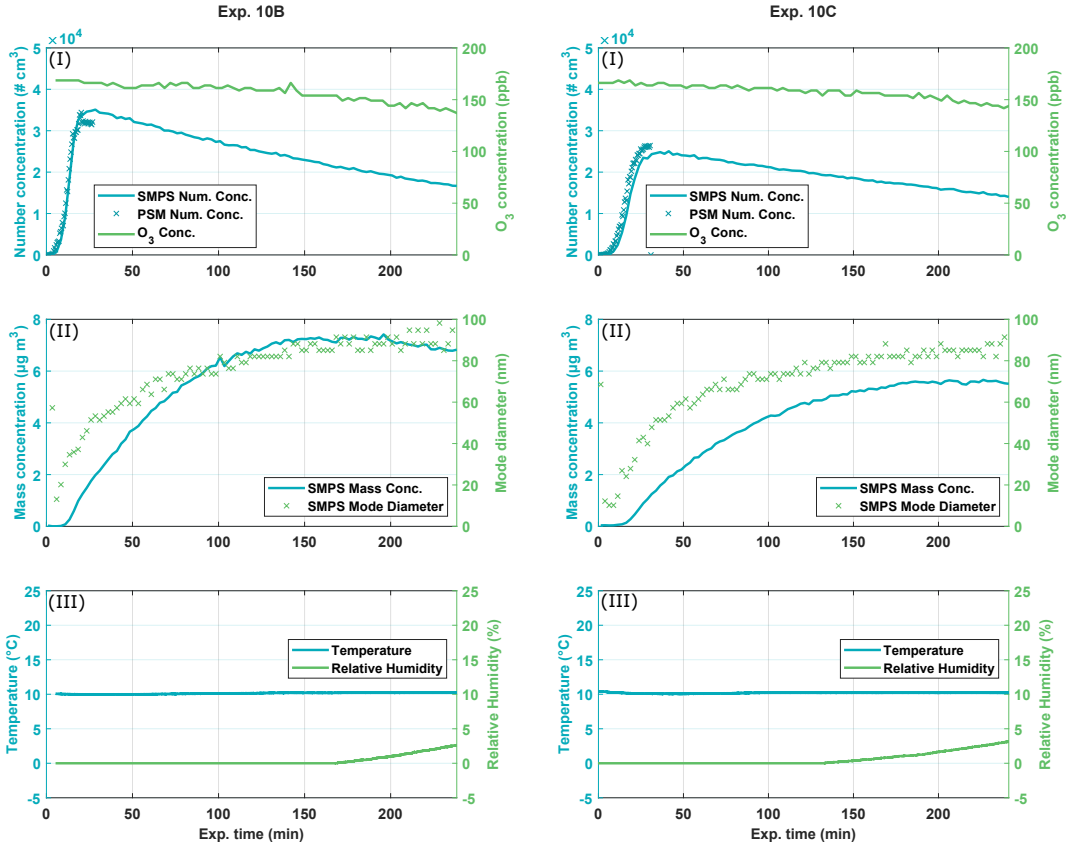

Figure S.5 **(I)** SMPS particle number concentration in # cm^{-3}, PSM particle number concentration in # cm^{-3}, and ozone concentration in ppb. **(II)** SMPS mass concentration in µg m^{-3} and SMPS mode diameter in nm. **(III)** Temperature in °C and relative humidity in %.

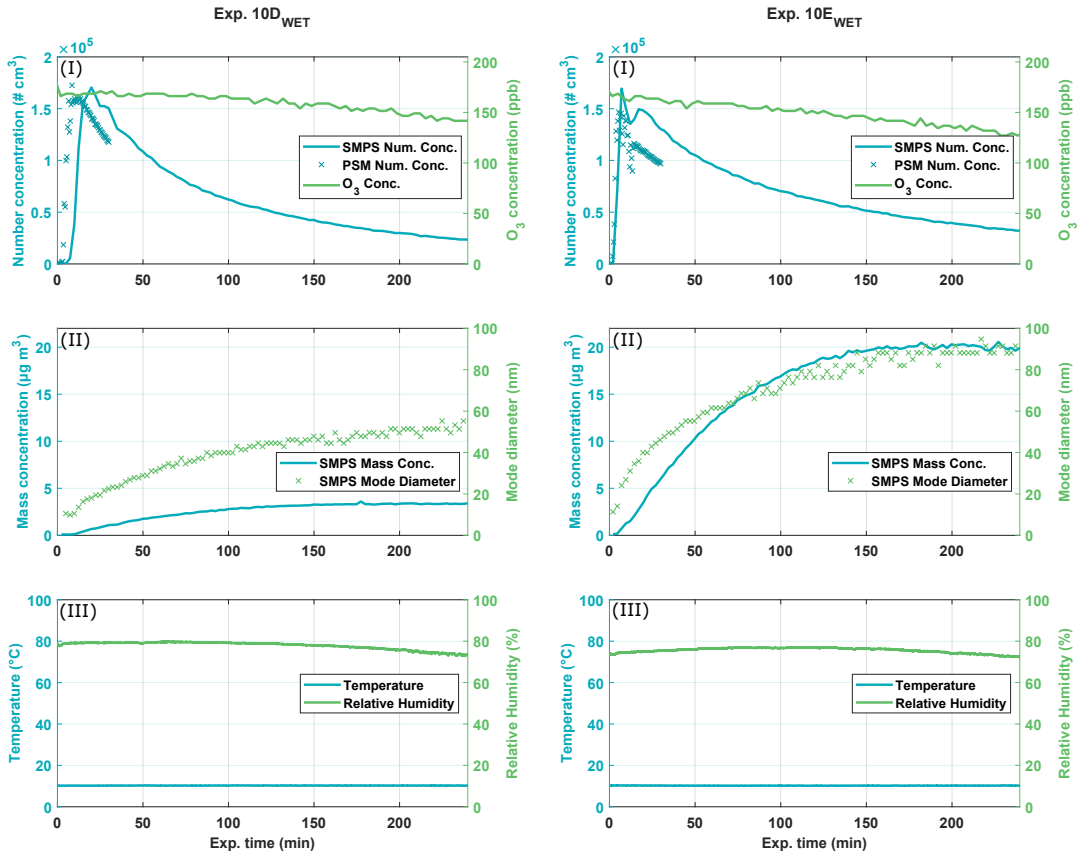

Figure S.6 (I) SMPS particle number concentration in # cm^{-3}, PSM particle number concentration in # cm^{-3}, and ozone concentration in ppb. **(II)** SMPS mass concentration in µg m^{-3} and SMPS mode diameter in nm. **(III)** Temperature in °C and relative humidity in %.

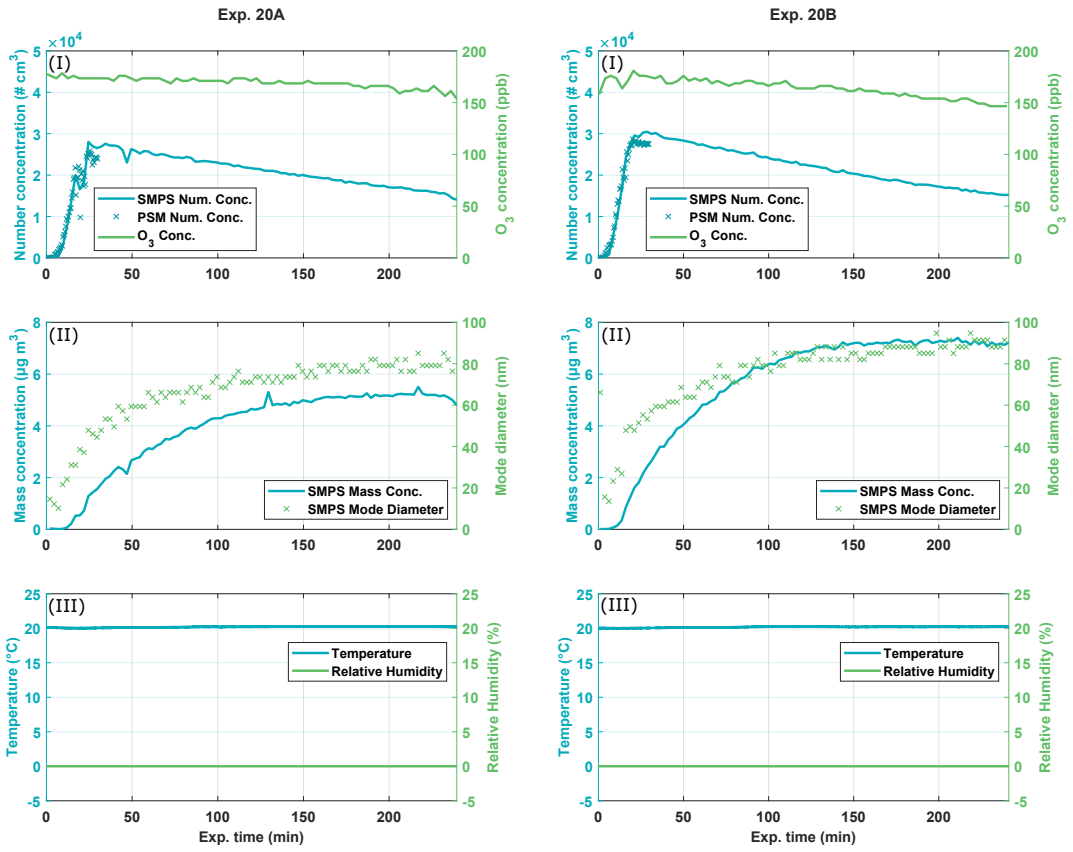

Figure S.7 **(I)** SMPS particle number concentration in # cm^{-3}, PSM particle number concentration in # cm^{-3}, and ozone concentration in ppb. **(II)** SMPS mass concentration in µg m^{-3} and SMPS mode diameter in nm. **(III)** Temperature in °C and relative humidity in %.

SI-4 Background concentration of sulfuric acid

Despite cleaning processes and flushing with clear air before all experiments, there are background concentrations of inorganic constituents, e.g. H_2SO_4. Sulfuric acid is considered a prime driver of new particle formation [5] and small background levels of sulfuric acid may play a role in the nucleation in the AURA chamber. Figure S.8 shows the sulfuric acid concentration measured with the NO_3-CIMS for experiments 10B, 10D, and 10E. Experiment 10B is performed at a RH of 0 % and experiments 10D and 10E were performed at a RH of 80 %. The concentration of sulfuric acid is very low at about 10^{-3} ppt.

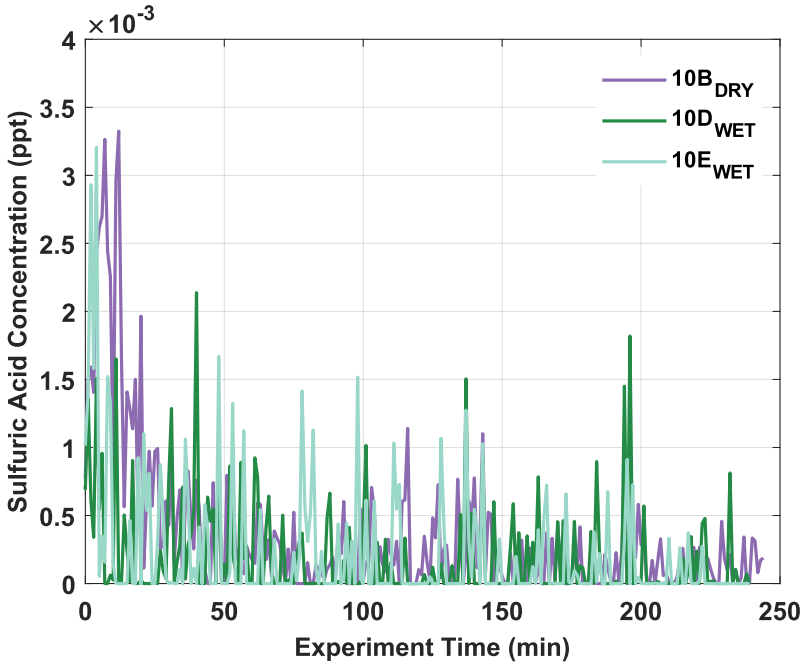

Figure S.8 Concentration of sulfuric acid in ppt measured with NO_3-CIMS for experiments 10B, 10D, and 10E.

SI-5 Evolution of moderately oxygenated species

The effect of relative humidity in moderately oxygenated species ($C_{10}H_{16}O_{2-5}$) from the FIGAERO-CIMS is investigated. No clear effect of increasing relative humidity is observed. The variability in the compounds in experiments 10B, 20B and 10D is correlated with the change in the total SMPS mass concentration. The large signals in experiment 10E arise as it is conducted with 20 ppb Δ^3-carene, whereas the remaining experiments were conducted with 10 ppb Δ^3-carene.

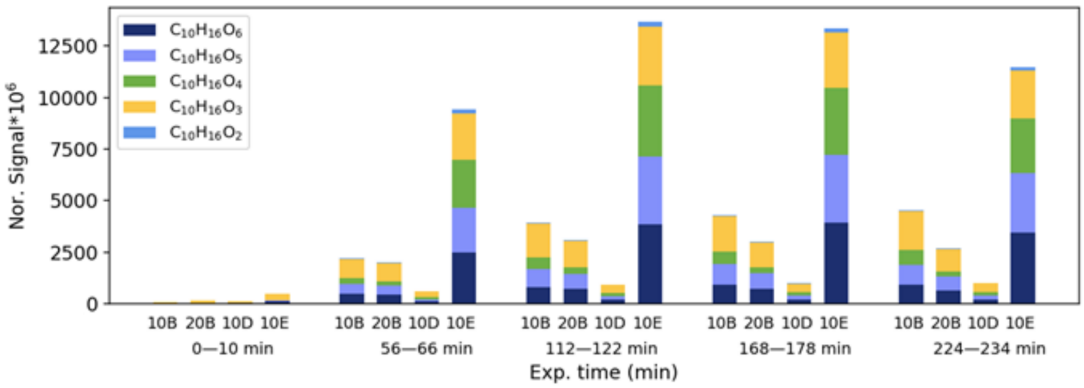

Figure S.9 Distribution of moderately oxygenated compounds ($C_{10}H_{16}O_{2-5}$) in experiments 10B, 20B, 10D, and 10 E.

SI-6 Offline Analysis

SI-6.1 Methods for UHPLC-QTOF-MS analysis

The LC systems were an ultra-high performance liquid chromatograph (UHPLC) (Dionex UltiMate 3000, Thermo Fisher). The HPLC stationary phase was an UPLC HSS T3 (AQUITY HSS T3, 2.1 × 100*mm*, 1.8 µm; Waters). The LC method is as follows: The flow rate is 0.3 mL min^{-1}, the column temperature is 45 °C, and the injection volume is 2 µL. The eluents are: A) 0.1 % acetic acid in MilliQ water and B) 0.1 % acetic acid in acetonitrile. From 0 to 2 minutes, the fraction of B is 0 %. From 2 to 10 minutes, the fraction of B is increased linearly from 0 % to 30 %. From 10 to 15 minutes, the fraction of B is increased linearly to 95 % and held constant for 3 minutes. From 18 to 19 minutes, the fraction of B is decreased to 0 %. The system is equilibrated between each run with 100 % A for 2 minutes. The mass spectrometer was operated in negative ionisation mode (ESI-) with the following conditions: Nebuliser pressure at 2 bar, dry gas flow at 19 L min^{-1}, dry gas temperature at 200 °C, capillary voltage at 3500 V, end plate offset of 500 V and a transfer time of 70 µs. The detection limits for the surrogate standards were 5.3 ng m^{-3} for *cis*-pinic acid, 3.1 ng m^{-3} for *cis*-pinonic acid, and 11.6 ng m^{-3} for diaterpenylic acid acetate.

SI-6.2 Time-evolution in *cis*-3-caric acid and *cis*-3-caronic acid

The time-evolution of the ozonolysis products *cis*-3-caric acid and *cis*-3-caronic acid. They are two of the main ozonolysis products from Δ^3-carene [4, 6, 7]. These data are from experiments 0A, 10A, 10B, 10C, and 20A. The data from experiment 20B was sadly lost due to an extraction error.

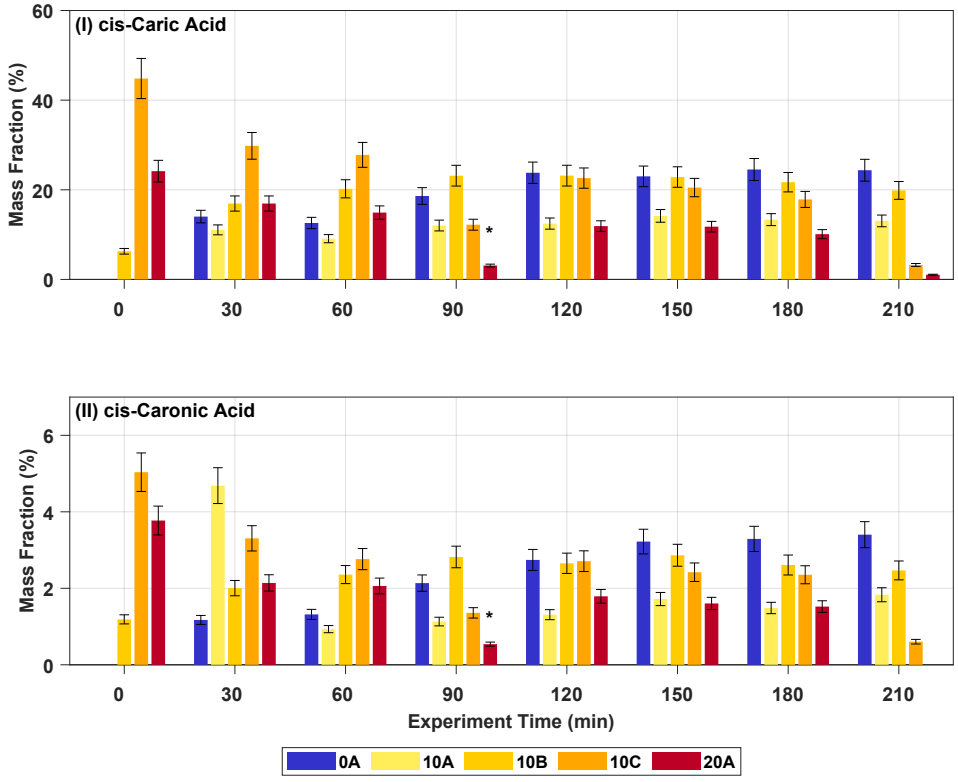

Figure S.10 Mass fractions of ozonolysis products of Δ^3-carene at 0, 10, and 20 °C. **(I)** The evolution over time of *cis*-3-caric acid in µg m^{-3} with an estimated uncertainty of ±10 %. **(II)** The evolution over time of *cis*-3-caronic acid in µg m^{-3} with an estimated uncertainty of ±10 %. *Low concentration due to incomplete extraction.

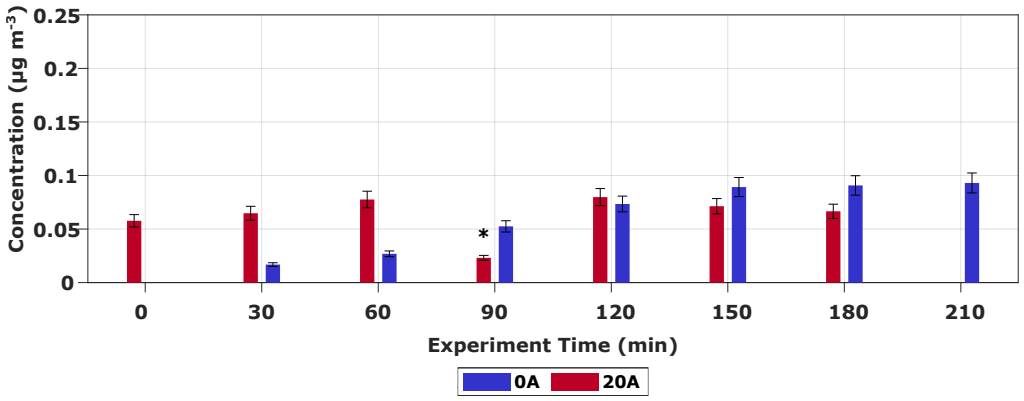

Figure S.11 Concentration of *cis*-caronic acid in $\mu g\,m^{-3}$ in experiments 0A and 20A. The uncertainty is estimated to $\pm 10\,\%$. *Low concentration due to incomplete extraction.

SI-6.3 Time-evolution in OH-caronic acid and MW170

The time-evolution of the ozonolysis products OH-3-caronic acid and MW170. These data are from experiments 0A, 10A, 10B, 10C, and 20A in Figure S.12 and from 10A, 10B, 10C, 10D, and 10E in Figure S.13. The data from experiment 20B was sadly lost due to an extraction error.

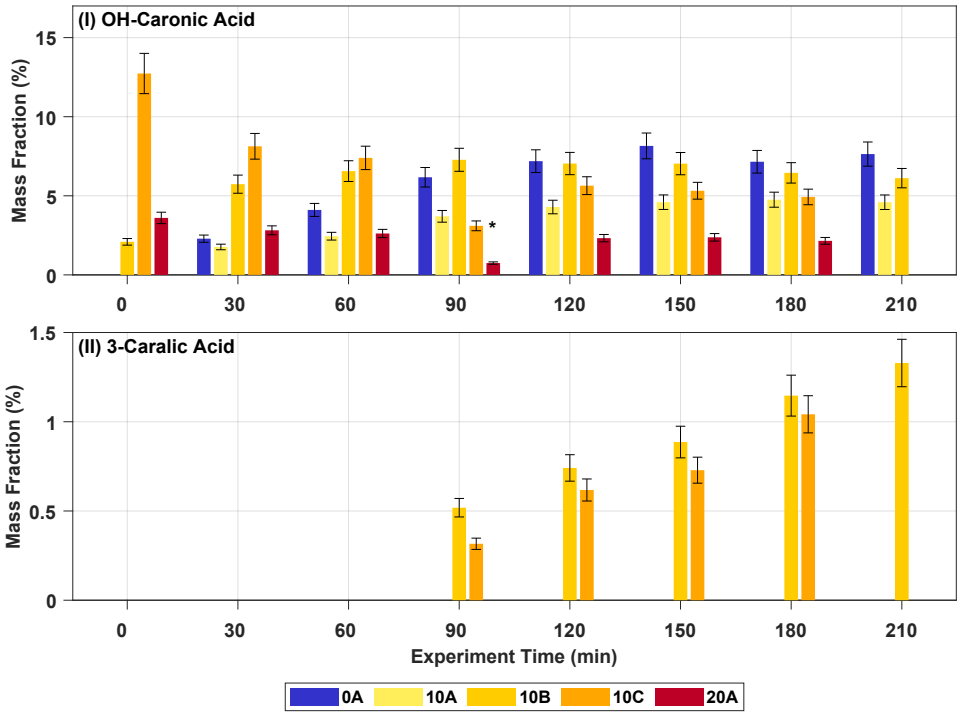

Figure S.12 Mass fractions of ozonolysis products of Δ^3-carene at 0, 10, and 20 °C. **(I)** The evolution over time of OH-3-caronic acid in $\mu g\,m^{-3}$ with an estimated uncertainty of ±10 %. **(II)** The evolution over time of MW170 in $\mu g\,m^{-3}$ with an estimated uncertainty of ±10 %.

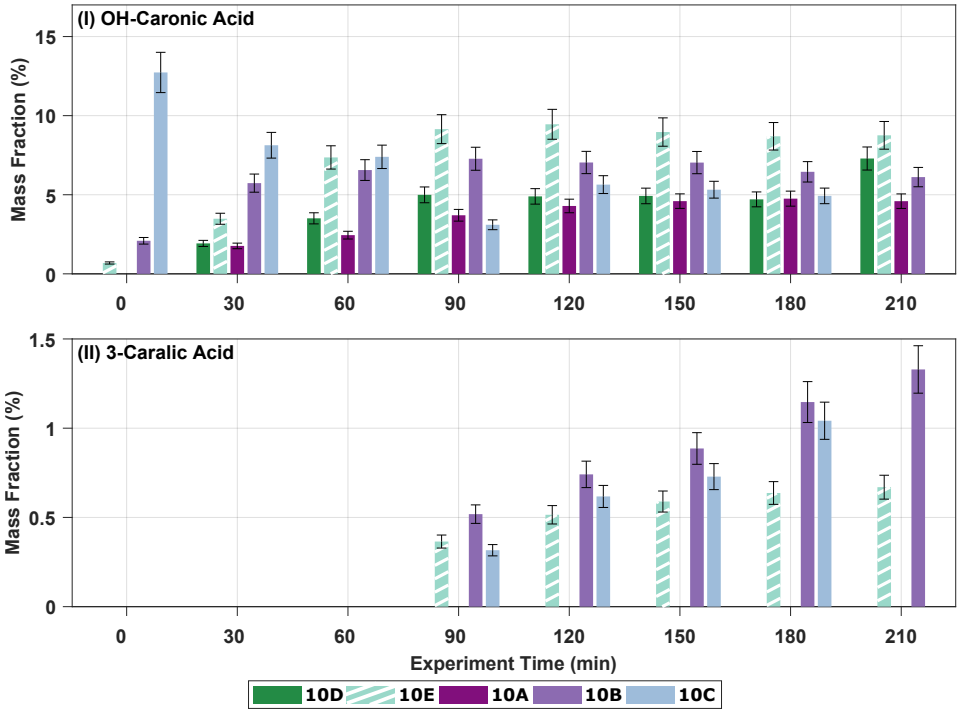

Figure S.13 Mass fractions of ozonolysis products of Δ^3-carene at 0, 10, and 20 °C. **(I)** The evolution over time of OH-3-caronic acid in µg m^{-3} with an estimated uncertainty of ±10 %. **(II)** The evolution over time of MW170 in µg m^{-3} with an estimated uncertainty of ±10 %.

SI-7 ADCHAM model results for experiment 0A, 20A, and 20B

Experiments 0A, 20A, and 20B also show good agreement between the modelled and measured ozone concentrations as well as the SOA mass concentration within the experimental uncertainties. Table S.1 shows the modelled SOA yields for experiments 0A, 10A, 10B, 20A and 20B.

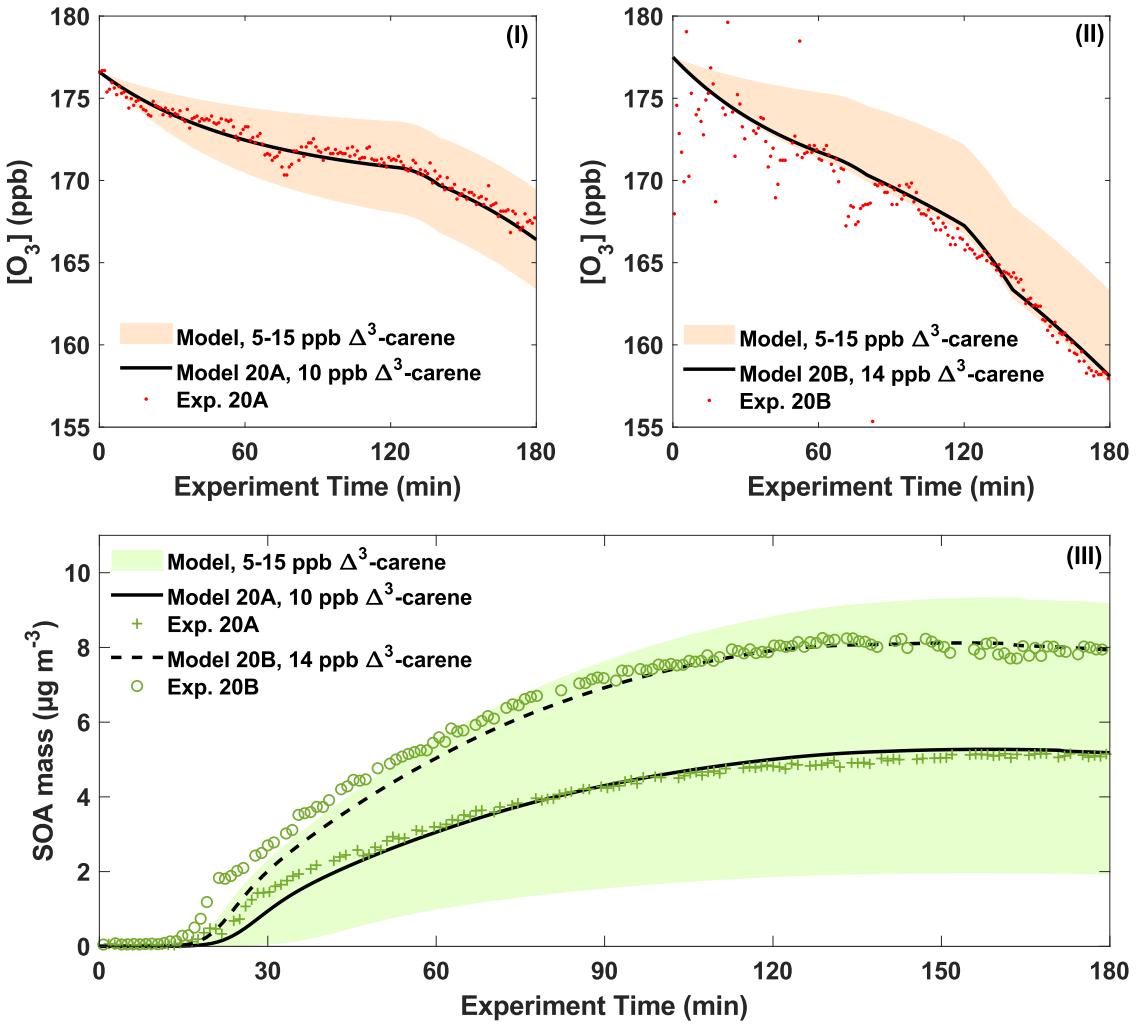

Figure S.14 (I, II) Measured and modelled ozone concentrations in experiments 20A and 20B. The ozone concentrations were used to calculate initial Δ^3-carene concentrations of 10 ppb and 14 ppb for experiments 20A and 20B respectively. **(III)** The measured and modelled SOA mass concentrations for experiments 20A and 20B. The model assumes initial concentrations as calculated from the ozone concentrations.

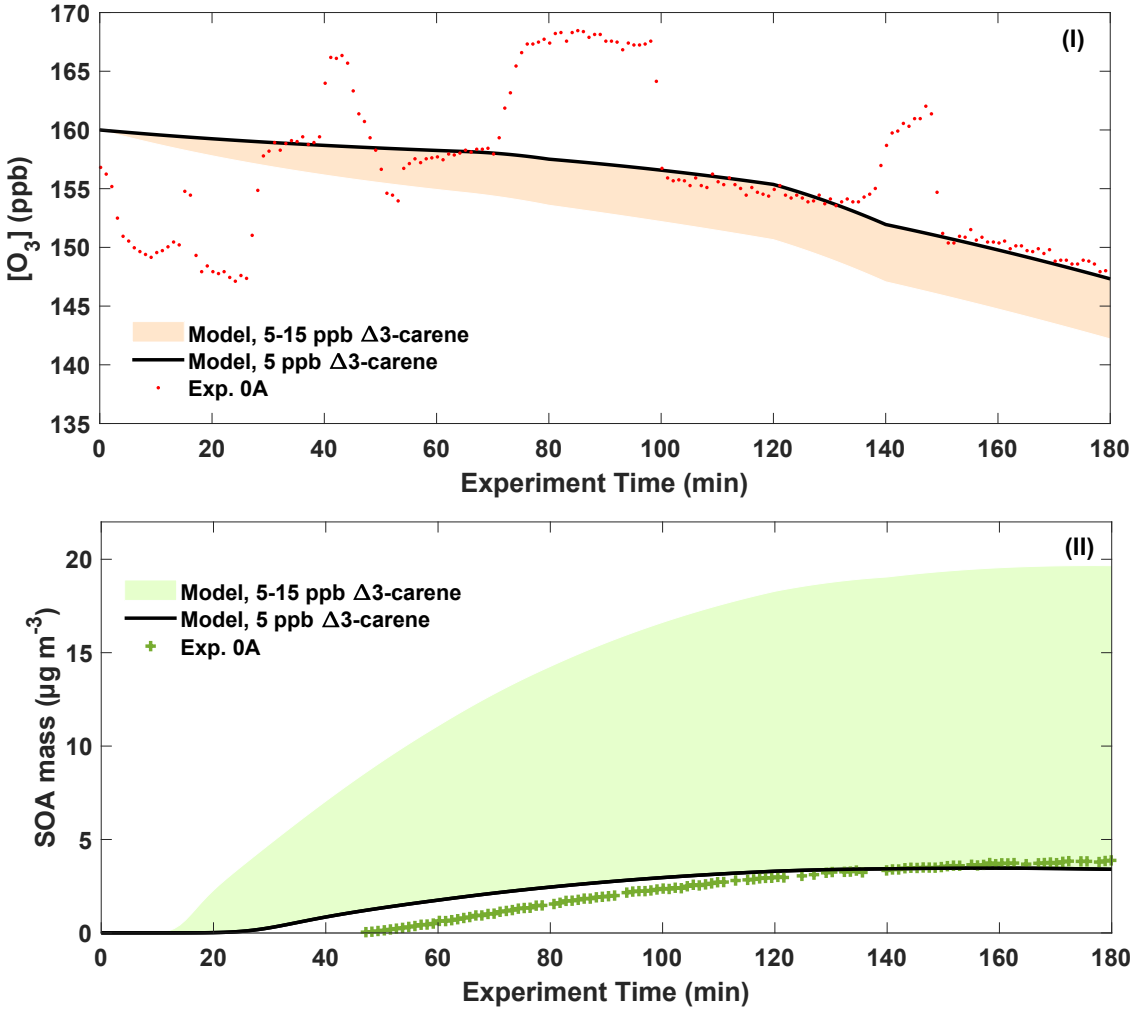

Figure S.15 **(I)** Measured and modelled ozone concentrations in experiment 0A. The ozone concentration was used to calculate initial Δ^3-carene concentrations of 5 ppb. **(II)** The measured and modelled SOA mass concentration for experiment 0A. The model assumes initial concentrations as calculated from the ozone concentrations.

Table S.1 Modelled maximum SOA mass yields for experiments 0A, 10A, 10B, 20A and 20B.

ID	SOA Yield (%)					
	No wall loss correction[a]	Wall loss corrected[a]	Ideal experiment[a,c]	No wall loss correction[b]	Wall loss corrected[b]	Ideal experiment[b,c]
0A	14.9	16.9	27.3	23.0	25.1	32.1
10A	12.2	13.7	21.2	16.4	18.1	23.6
10B	18.6	20.2	25.6	15.5	17.1	23.7
20A	9.9	11.1	16.3	9.9	11.1	16.3
20B	12.2	13.2	18.2	9.4	10.4	16.4

[a] SOA yield from simulations using an initial Δ^3-carene concentration that gives optimal agreement between the modelled and observed O_3 concentrations in the AURA chamber (Figure 5 and Figure S.14-15). For Exp. 0A, 10A, 10B, 20A and 20B this was 5, 6.5, 14, 10, and 14 ppb, respectively.
[b] SOA yields from simulations using an initial Δ^3-carene concentration of 10 ppb for all experiments.
[c] Ideal experiments without gas and particle wall losses and chamber dilution because of instruments sampling.

References

(1) R. K. Pathak, C. O. Stanier, N. M. Donahue and S. N. Pandis, Ozonolysis of α-pinene at atmospherically relevant concentrations: Temperature dependence of aerosol mass fractions (yields), *Journal of Geophysical Research: Atmospheres*, 2007, **112**, DOI: https://doi.org/10.1029/2006JD007436.

(2) K. Kristensen, L. N. Jensen, M. Glasius and M. Bilde, The effect of sub-zero temperature on the formation and composition of secondary organic aerosol from ozonolysis of alpha-pinene, *Environ. Sci.: Processes Impacts*, 2017, **19**, 1220–1234.

(3) K. Kristensen, L. N. Jensen, L. L. J. Quéléver, S. Christiansen, B. Rosati, J. Elm et al., The Aarhus Chamber Campaign on Highly Oxygenated Organic Molecules and Aerosols (ACCHA): particle formation, organic acids, and dimer esters from α-pinene ozonolysis at different temperatures, *Atmospheric Chemistry and Physics*, 2020, **20**, 12549–12567.

(4) D. Thomsen, J. Elm, B. Rosati, J. T. Skønager, M. Bilde and M. Glasius, Large Discrepancy in the Formation of Secondary Organic Aerosols from Structurally Similar Monoterpenes, *ACS Earth and Space Chemistry*, 2021, **5**, 632–644.

(5) M. Sipilä, T. Berndt, T. Petäjä, D. Brus, J. Vanhanen, F. Stratmann et al., The Role of Sulfuric Acid in Atmospheric Nucleation, *Science*, 2010, **327**, 1243–1246.

(6) M. Glasius, M. Lahaniati, A. Calogirou, D. Di Bella, N. R. Jensen, J. Hjorth, D. Kotzias and B. R. Larsen, Carboxylic Acids in Secondary Aerosols from Oxidation of Cyclic Monoterpenes by Ozone, *Environmental Science & Technology*, 2000, **34**, 1001–1010.

(7) D. Thomsen, L. D. Thomsen, E. M. Iversen, T. N. Björgvinsdóttir, S. F. Vinther, J. T. Skønager, T. Hoffmann, J. Elm, M. Bilde and M. Glasius, Ozonolysis of α-Pinene and Δ^3-Carene Mixtures: Formation of Dimers with Two Precursors, *Environmental Science & Technology*, 2022, **56**, 16643–16651.